^{1}H NMR Studies of Human Lysozyme: Spectral Assignment and Comparison with Hen Lysozyme†

Christina Redfield* and Christopher M. Dobson

Oxford Centre for Molecular Sciences and Inorganic Chemistry Laboratory, University of Oxford, South Parks Road, Oxford OX1 3QR, England

Received November 28, 1989; Revised Manuscript Received March 29, 1990

ABSTRACT: Complete main-chain (NH and αCH) ^{1}H NMR assignments are reported for the 130 residues of human lysozyme, along with extensive assignments for side-chain protons. Analysis of 2-D NOESY experiments shows that the regions of secondary structure for human lysozyme in solution are essentially identical with those found previously in a similar study of hen lysozyme and are in close accord with the structure of the protein reported previously from X-ray diffraction studies in the crystalline state. Comparison of the chemical shifts, spin–spin coupling constants, and hydrogen exchange behavior are also consistent with closely similar structures for the two proteins in solution. In a number of cases specific differences in the NMR parameters between hen and human lysozymes can be correlated with specific differences observed in the crystal structures.

The NMR[1] resonance assignments for main-chain protons of 125 of the 129 residues of hen egg white lysozyme were reported in 1988 (Redfield & Dobson, 1988). Since then, the resonances of all the remaining 4 residues (R68, R73, N103, and N106) have been identified (unpublished results). In addition, assignments of some 280 side-chain protons, representing about 70% of the total, have so far been determined. Although resonance assignments for many proteins including plastocyanin, cytochrome *c*, and staphylococcal nuclease have now been reported, this enzyme of molecular weight 14 500 is still one of the largest proteins for which such a complete level of ^{1}H assignments has been achieved without the use of isotopic enrichment and heteronuclear 2-D and 3-D NMR techniques (Driscoll et al., 1987; Chazin & Wright, 1988; Wand et al., 1989; Gao et al., 1989; Torchia et al., 1989). The existence of these assignments is permitting the extensive study of the structure, dynamics, and behavior of the protein in solution.

Human lysozyme is found in a variety of secretions including milk, tears, and saliva and differs from hen lysozyme in about 40% of its sequence (Imoto et al., 1972). These differences include 51 amino acid substitutions and the insertion of a glycine at position 48. Assignments for side-chain resonances from 38 of the 130 amino acid residues of human lysozyme have already been reported (Boyd et al., 1985). These assignments were achieved by using a combination of one- and two-dimensional NMR techniques, utilizing in particular through-space NOE connectivities analyzed with reference to the X-ray structure at 1.5-Å resolution (Artymiuk & Blake, 1981). In the present paper the complete main-chain assignments for human lysozyme are presented along with assignments for many side-chain protons which include confirmation of the earlier results. These were made by sequential methods completely independently of the hen lysozyme assignments and without reference to the X-ray structure.

The assignment of the human lysozyme spectrum is of particular interest because high-resolution X-ray structures of hen and human lysozymes show that these two proteins have very similar structures in the solid state; an RMS difference of 0.74 Å is obtained for the α carbon atoms (Artymiuk, & Blake, 1981). Comparison of NMR parameters including observed NOE effects, hydrogen exchange rates, coupling constants, and chemical shifts will provide information about similarities and differences in the solution structures of these two homologous proteins. Conversely, the influence of amino acid changes on the observed NMR parameters can then be analyzed by comparison with the results of the crystallographic studies.

Both hen and human lysozymes have recently been the subject of studies involving site-specific mutagenesis directed at understanding the catalytic activity, substrate specificity, and stabilities of the two proteins (Muraki et al., 1987, 1989; Kikuchi et al., 1988; Archer et al., 1990). NMR techniques have the potential to define changes in conformation associated with such mutations. It is clearly essential that the spectra are assigned and that both the spectrum of the native proteins and the changes which result from amino acid substitutions are understood in detail. The present work, therefore, forms the basis for studies of this type.

Materials and Methods

Human lysozyme was obtained from Sigma Chemical Co. and was dialyzed at pH 3 before use. NMR samples were 5 mM in lysozyme at pH 3.8, and experiments were run at 35 °C.

† This work was supported by the U.K. Science and Engineering Research Council.

[1] Abbreviations: NMR, nuclear magnetic resonance; 2-D, two dimensional; COSY, two-dimensional *J*-correlated spectroscopy; RELAY, two-dimensional relayed coherence transfer spectroscopy; NOE, nuclear Overhauser enhancement; NOESY, two-dimensional NOE spectroscopy; TOCSY, two-dimensional total coherence spectroscopy; E.COSY, exclusive correlation spectroscopy; type J, amino acid residue belonging to the group consisting of Trp, Tyr, Phe, His, Asp, Asn, Cys, and Ser; type U, amino acid residue belonging to the group consisting of Lys, Arg, Met, Gln, Glu, Leu, and Ile; type X, any of the 20 common amino acid residues; $d_{NN}(i,j)$, NOE connectivity between the NH proton on residue *i* and the NH proton on residue *j*; $d_{\alpha N}(i,j)$, NOE connectivity between the αCH proton on residue *i* and the NH proton on residue *j*; $d_{\beta N}(i,j)$, NOE connectivity between the βCH proton on residue *i* and the NH proton on residue *j*; d_{NN}, $d_{NN}(i,i+1)$; $d_{\alpha N}$, $d_{\alpha N}(i,i+1)$; $d_{\beta N}$, $d_{\beta N}(i,i+1)$; *J*, coupling constant; RMS, root mean square.

0006-2960/90/0429-7201$02.50/0

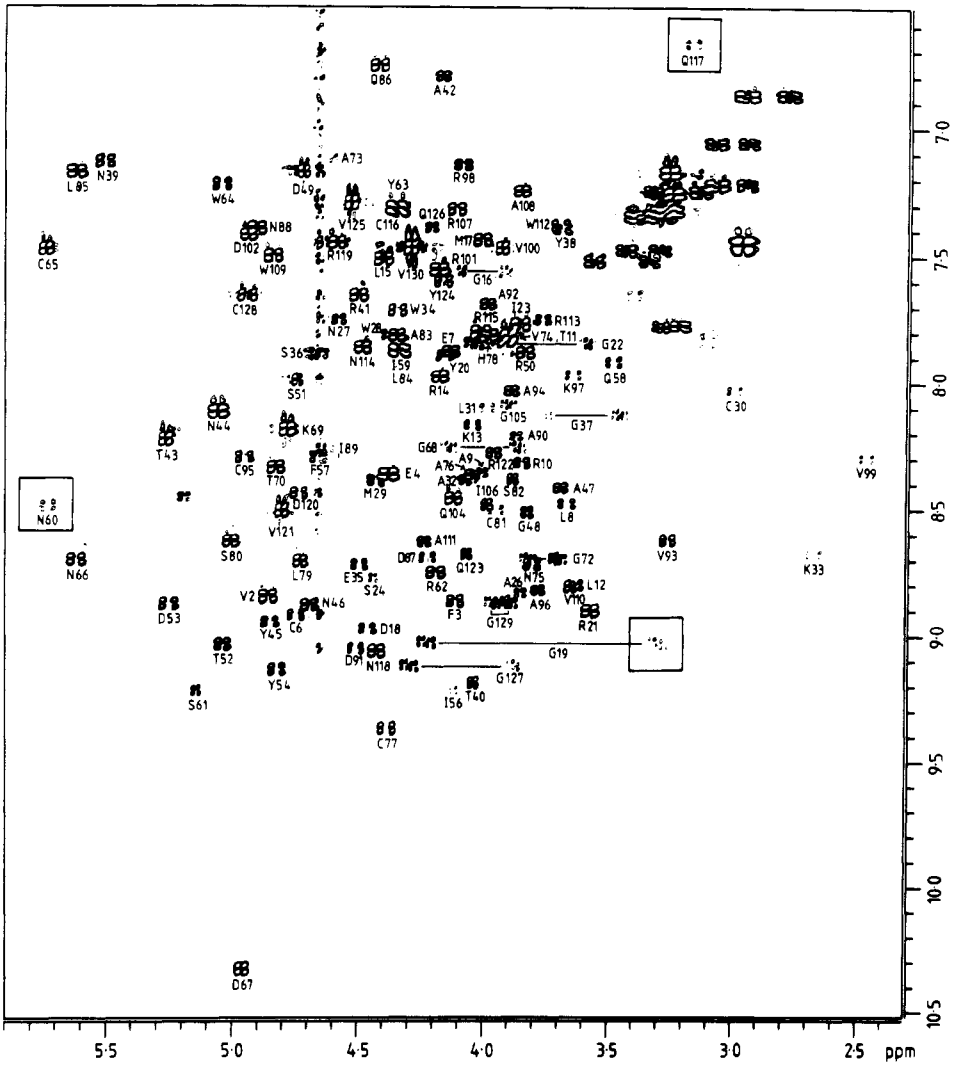

FIGURE 1: Fingerprint region of the phase-sensitive 500-MHz pre-TOCSY COSY spectrum of nonexchanged human lysozyme. Both positive and negative contour levels are plotted; cross peaks in boxes are plotted at a lower level. Cross peaks from R5, L25, and G55 are not seen. The cross peaks of G55 are visible in the COSY spectrum of human lysozyme collected in D_2O.

Table I: Summary of COSY, RELAY, and Double-RELAY Information Used for Spin System Classification[a]

	COSY			RELAY			double-RELAY
residue	NH–αCH	αCH–βCH	βCH–γCH	NH–βCH_3	NH–βCH	αCH–γCH_3	NH–γCH_3
alanine				all			
threonine	40, 52	40	40		11, 43, 70	11, 43, 52, 70	11, 43, 52, 70
valine	99, 100				2, 74, 93, 110, 121, 125, 130	all	2, 74, 93, 110, 121, 125, 130
isoleucine	56, 89, 106	89	89		23, 59	23, 56, 59, 106	23, 59

[a] Residue numbers for each amino acid type are listed in the column that corresponds to the particular type of cross peak observed. Information about COSY peaks is only given when RELAY and double-RELAY peaks were not observed.

All NMR experiments were performed on a home-built 500-MHz spectrometer equipped with an Oxford Instruments Co. magnet, a GE/Nicolet 1280 computer and 293D pulse programmer, and a Bruker probe. Phase-sensitive *J*-correlated spectroscopy (COSY) (Aue et al., 1976; Bax & Freeman, 1981), single and double relayed coherence transfer spectroscopy (RELAY) (Eich et al., 1982; Bax & Drobny, 1985), and nuclear Overhauser enhancement spectroscopy (NOESY) (Jeener et al., 1979; Anil Kumar et al., 1980) experiments used for assignment were performed according to the method of States et al. (1982) and with standard phase-cycling schemes. Data sets consisting of 512 t_1 increments of 32, 48, and 64 transients were collected for the COSY, RELAY, and double-RELAY experiments, respectively. Data sets consisting of 256 t_1 increments of 32 transients were collected for the NOESY experiments. In all cases a sweep width of 6024 Hz was used in both dimensions. Solvent suppression in 90% H_2O/10% D_2O samples was achieved by a 0.8–1.0-s presaturation of the water resonance. In RELAY and double-RELAY experiments mixing periods (2τ) of 36 ms were used. Mixing times of 150 or 200 ms which were randomly varied by 10% were used in NOESY experiments (Macura et al., 1981). All spectra were resolution enhanced in t_2 by trapezoidal multiplication and double-exponential multiplication. NOESY spectra were not resolution enhanced in t_1. All other spectra were resolution enhanced in t_1 by trapezoidal multiplication. After zero filling in both the t_1 and t_2 dimensions the digital resolution was 3.0 Hz/point.

In some COSY and NOESY experiments a 25-ms MLEV-17 (Bax & Davies, 1985) sequence was inserted im-

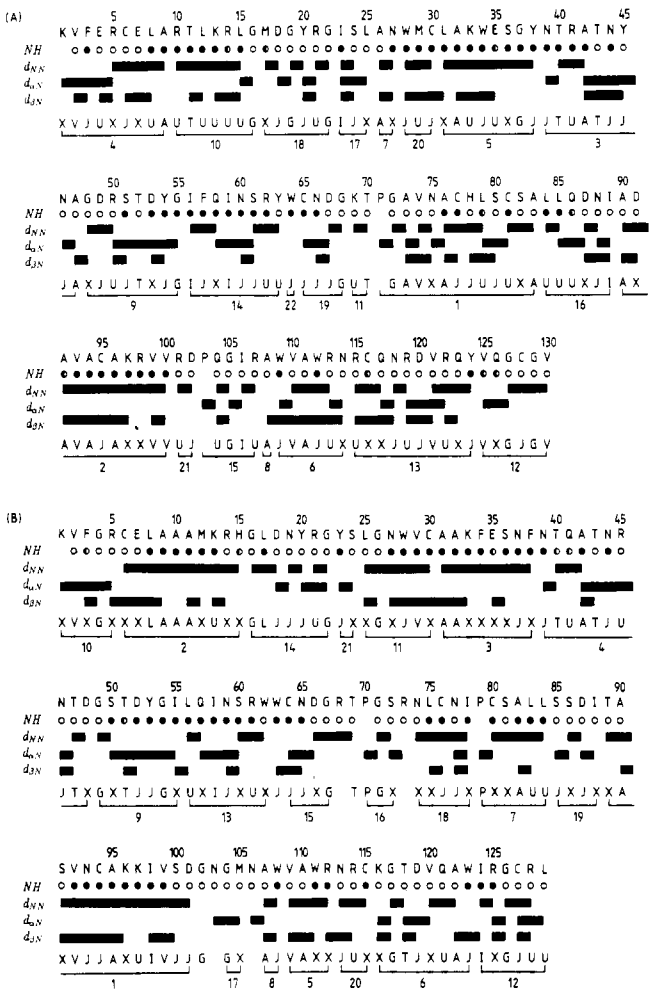

FIGURE 2: Amino acid sequence, summary of hydrogen exchange rates, and summary of the NOE connectivities used in the sequential assignment procedure for (A) human and (B) hen lysozymes. Filled, half-filled, and empty circles indicate amides with slow, intermediate, and rapid exchange rates, respectively (Redfield & Dobson, 1988). Peptide segments identified in the assignment procedure and the amino acid types of the residues in these segments are shown. The numbers beneath these segments indicate the order in which they were assigned.

mediately after the first 90° pulse following the procedure introduced by Otting and Wüthrich (1987). Insertion of this isotropic mixing period before the t_1 period lessens the bleaching of αCH resonances around the water peak which usually occurs when presaturation of the water peak is used for solvent suppression. These pre-TOCSY COSY and NOESY spectra were collected and processed as described above.

All spectra are presented as contour plots. In COSY spectra both positive and negative levels are shown; in NOESY spectra only positive levels are shown. The contours are spaced logarithmically, so that the nth level corresponds to an intensity of 0.7^n times the chosen scaling factor. In all spectra presented here the horizontal and vertical axes represent F_1 and F_2, respectively.

NH–αCH coupling constants for non-glycine residues were measured from COSY data sets of 512 t_1 increments of 32 transients. Good digital resolution was achieved in the F_2 dimension by collecting FID's of 4096 complex points. A sweep width of 5405.40 Hz was used in both dimensions. The spectra were processed as described above. After zero filling once in the t_2 dimension the digital resolution was 0.66 Hz/point. NH–αCH coupling constants for glycine residues were measured from exclusive correlation spectroscopy (E.COSY)

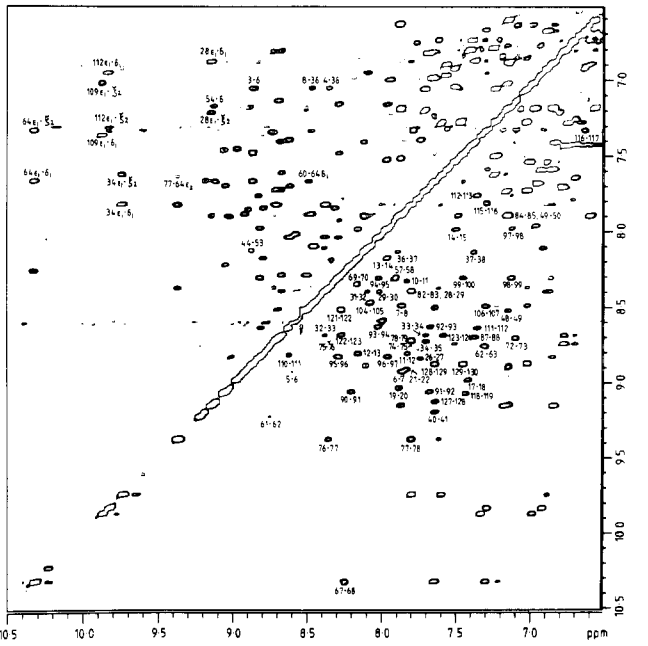

FIGURE 3: NH and aromatic region of the phase-sensitive 500-MHz pre-TOCSY NOESY spectrum of nonexchanged human lysozyme, τ_m = 200 ms. Connectivities involving pairs of neighboring NH protons are labeled in the region below the diagonal. Long-range d_{NN} connectivities and NH–aromatic connectivities are labeled in the region above the diagonal.

data sets of 512 t_1 increments of 24 transients (Griesenger et al., 1987). CYCLOPS phase cycling for the removal of quadrature images was omitted in order to shorten the acquisition time for the experiment.

NH–αCH coupling constants can be measured from the antiphase splitting in cross sections parallel to F_2 through the NH–αCH fingerprint region cross peaks in COSY spectra (Marion & Wüthrich, 1983). However, as the amide line width increases relative to the coupling constant, distortions occur in antiphase cross peaks; the overlap of positive and negative cross peak components leads to cancellation of signal at the center of the cross peak and gives an observed splitting which is greater than the true coupling constant (Neuhaus et al., 1985). In this study the distortions arising from the finite amide line width were corrected for by using spectral simulations. Cross sections parallel to F_2 through the NH–αCH cross peak were fitted to cross sections simulated by applying appropriate resolution enhancement functions to antiphase Lorentzian doublets. The fits were done by using the downhill simplex method (Press et al., 1986); the parameters fitted were coupling constant, line width, and chemical shift.

Coupling constants for glycine residues were obtained from E.COSY spectra (Griesenger et al., 1987). The fitting procedure described above was used to extract the active coupling constant, line width, and chemical shift from each antiphase cross section. The passive coupling constant was obtained by measuring the displacement of the centers of cross sections within a cross peak; this displacement was measured in the simulation by the difference in chemical shift found in the fits of individual cross sections within each cross peak.

In this study several NMR parameters measured experimentally are compared with parameters calculated by using the X-ray diffraction structures of lysozyme. The structure of tetragonal human lysozyme crystals has been refined at 1.5-Å resolution (Artymiuk & Blake, 1981). The structure of tetragonal hen lysozyme crystals has been refined at 2.0-Å resolution (Blake et al., 1967; Handoll, 1985). Hydrogen atom positions were generated from the heavy atom coordinate sets

by using the program VNMR kindly provided by Dr. J. C. Hoch (Hoch, 1983); a C–H bond length of 1.08 Å and a N–H bond length of 1.0 Å were used.

Coupling constants were calculated from the crystal structure by using the Karplus equation (Karplus, 1959):

$$^3J_{N\alpha} = A \cos^2 \theta + B \cos \theta + C \qquad \theta = \phi + 60°$$

Values for A, B, and C of 6.4, −1.4, and 1.9 were used; these values were derived from a least-squares fit of the NH–αCH coupling constants of BPTI in solution and the crystallographic ϕ torsion angles (Pardi et al., 1984).

Ring current shift calculations were also carried by using the program VNMR (Hoch et al., 1982; Hoch, 1983). The shifts were calculated according to the procedure of Johnson and Bovey (1958) using ring current intensity factors of Giessner-Prettre and Pullman (1969). Other values for these factors are present in the literature, but the results of an earlier study of the methyl group chemical shifts of human lysozyme showed that the values of Giessner-Prettre and Pullman gave better agreement between experimental and calculated shifts (Boyd et al., 1985).

Secondary shifts for NH and αCH resonances were calculated by subtracting the random coil chemical shift values obtained by Bundi and Wüthrich (1979) for tetrapeptides from the observed chemical shifts; a positive number indicates a downfield shift while a negative value indicates an upfield shift. However, the random coil values of Bundi and Wüthrich for Trp, Tyr, Phe, and His were not used; the downfield NH and upfield αCH shifts of these four residues compared to others reflect the ring current contribution from the average position of the aromatic ring relative to the backbone atoms in the tetrapeptide. Instead, the random coil values of Leu are used for the aromatic residues and the contribution of the aromatic side chain to the shifts of the NH and αCH resonances is included in the calculation of the ring current shift.

Results and Discussion

(*a*) *Assignment of the Human Lysozyme Spectrum.* The fingerprint region of the COSY spectrum of human lysozyme is shown in Figure 1. The assignment of the NH–αCH cross peaks in this spectrum was carried out by the same procedure used for the earlier assignment of the hen lysozyme spectrum. The first stage involved the assignment of each fingerprint region cross peak to a particular amino acid type or to a more general class of amino acid types on the basis of COSY, RELAY, and double-RELAY spectra. The second stage involved the identification of sequential d_{NN}, $d_{\alpha N}$, and $d_{\beta N}$ connectivities in NOESY spectra. A detailed discussion of the procedure has been given in the hen lysozyme assignment paper (Redfield & Dobson, 1988).

Human lysozyme is composed of 130 amino acid residues including 2 proline residues and 11 glycine residues. The fingerprint region of the COSY spectrum of human lysozyme contains 10 pairs of cross peaks characteristic of glycine residues. The 11th glycine residue, identified at a later stage in the assignment process, has two αCH resonances with the same chemical shift and gives a cross peak similar to that of non-glycine residues. An additional 115 cross peaks characteristic of non-glycine residues have been identified in this region; cross peaks for 2 residues have, therefore, not been observed. Fingerprint region cross peaks of all the 14 alanine, 5 threonine, 9 valine, and 5 isoleucine residues of human lysozyme were identified by establishing a through-bond connectivity between the NH, αCH, and the methyl resonances using COSY, RELAY, and double-RELAY spectra. These

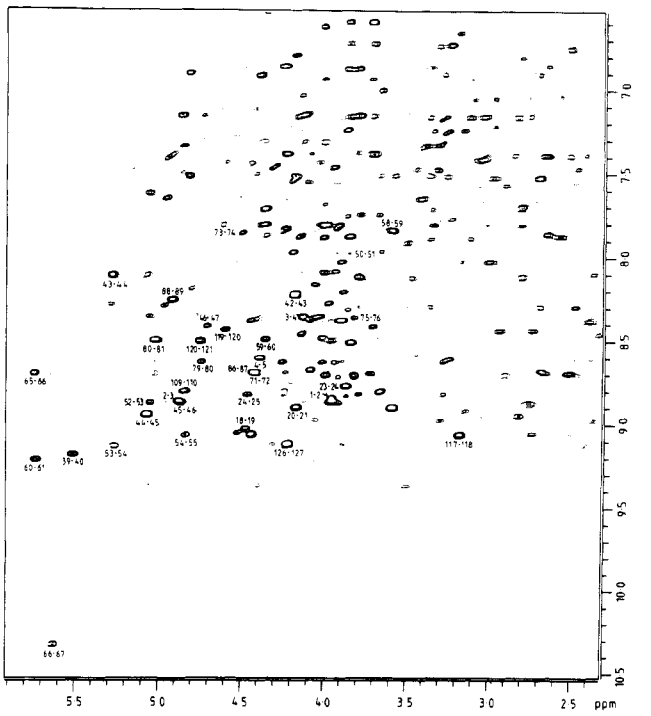

FIGURE 4: Phase-sensitive 500-MHz pre-TOCSY NOESY spectrum of nonexchanged human lysozyme, τ_m = 200 ms. Sequential $d_{\alpha N}$ connectivities identified in the assignment process are labeled.

data are summarized in Table I; full details of the procedure used have been described previously for hen lysozyme (Redfield & Dobson, 1988). The identification of NH–αCH cross peaks arising from glycine, alanine, threonine, valine, and isoleucine accounts for 43 of the fingerprint region cross peaks.

Eight types of amino acid residue (Asp, Asn, Tyr, His, Phe, Trp, Ser, Cys) have two βCH protons and no γCH protons; these are classified as type J. Six types of amino acid residue (Arg, Lys, Glu, Gln, Met, Leu) have two βCH protons coupled to one or two γCH protons; these are classified as type U. Distinction between type J and type U residues is not always straightforward because cross peaks to γCH protons are not always clearly observed. In order to make a division of the resonances, for which such a situation arises, into the two categories, chemical shift values were used. Residues with βCH resonances in the region downfield of 2.6 ppm were provisionally classified as type J and those with βCH resonances upfield of 2.3 ppm as type U (Redfield & Dobson, 1988). Type J and type U residues can be classified on this basis if NH–βCH RELAY peaks and unambiguous NH–αCH or αCH–βCH COSY cross peaks can be observed. Sixty-three of the anticipated 83 spin systems of these types of residue were identified in spectra of human lysozyme. The 20 remaining fingerprint region cross peaks are classified as type X, indicating that insufficient evidence is available at this stage to assign them to any particular group of amino acid residues.

The second stage of assignment involves the correlation of cross peaks in the fingerprint region with specific amino acid residues in the protein sequence (Wüthrich, 1986). As the molecular weight of a protein increases, so do the number of resonances and their line widths; hence, the overlap of cross peaks in the COSY spectrum. There are many cross peaks in the fingerprint region of the COSY spectrum of human lysozyme which share either the same NH or αCH chemical shift value. In the assignment study of hen lysozyme the use of NMR samples containing different subsets of amide hydrogens, generated by controlled exchange of protons for deuterons from D_2O solvent, was found to be a very useful

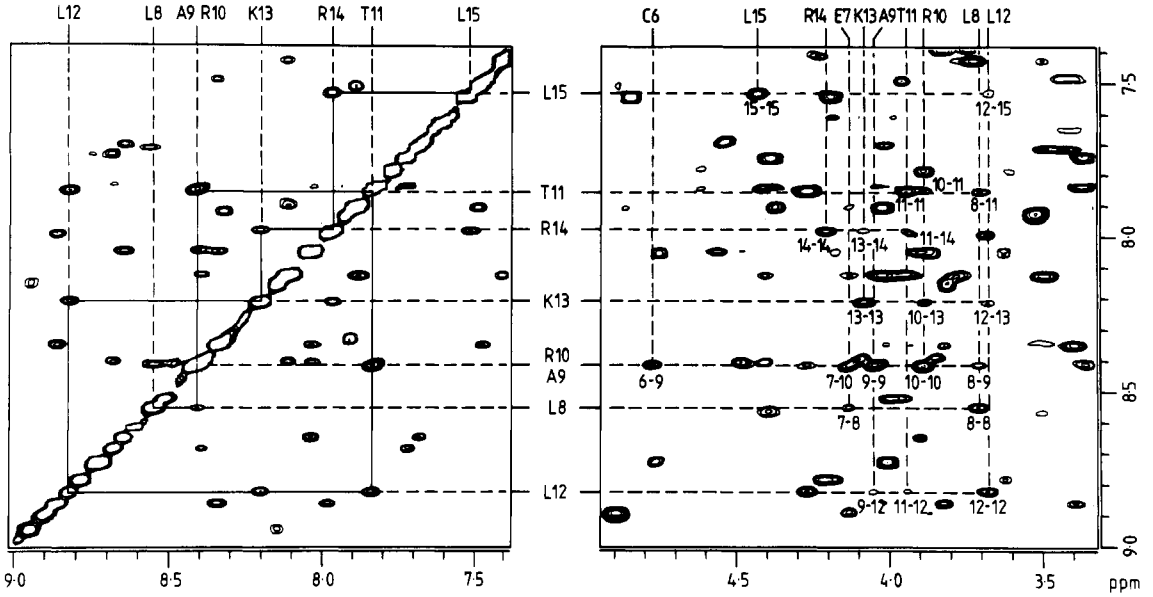

FIGURE 5: Phase-sensitive 500-MHz NOESY spectra for partly exchanged human lysozyme in D_2O. Sequential d_{NN} connectivities for residues 8–15 are shown on the left; $d_{\alpha N}(i,i)$, $d_{\alpha N}(i,i+1)$, and $d_{\alpha N}(i,i+3)$ connectivities for residues 6–15 are shown on the right.

method for obtaining spectral simplification and, therefore, decreasing spectral overlap (Redfield & Dobson 1988). Human lysozyme exhibits very similar hydrogen exchange behavior to that of hen lysozyme, see below, and this strategy for overcoming overlap was adopted in the present study. In the hen lysozyme assignment procedure it was also found to be helpful to identify first from sequential NOEs segments of the polypeptide chain that contained several easily identifiable amino acids such as glycine, alanine, threonine, valine, and isoleucine. Human lysozyme contains 44 of these easily identifiable residues distributed throughout the protein sequence shown in Figure 2A. When a large number of assignments have been made with these residues as starting points, then assignments can be based on the less specific type J and type U classification because of the restrictions on the length and sequence of the remaining stretches of unassigned amino acid residues.

Assignments for all 130 amino acid residues of human lysozyme were obtained from sequential NOE effects used in this way. The d_{NN} and $d_{\alpha N}$ effects used to make the assignments are shown in Figures 3 and 4. The assignments are based on 22 sequential peptide segments. The NOE connectivities observed, hydrogen exchange rates, and amino acid classifications are summarized in Figure 2A. The first 8 peptide segments assigned contain one or more alanine residues. Peptide segments 9–19 are assigned on the basis of the threonine, valine, isoleucine, and glycine residues they contain. The last three peptide segments are assigned on the basis of the number of residues they contain; at this stage of assignment only three small gaps in the sequence remain.

The human lysozyme assignments are summarized in Table II. In the light of these assignments further discussion of the type J and type U spin systems is possible. The spin systems assigned to Y63 and C81, both type J residues, had been provisionally classified as type U on the basis of βCH chemical shifts of 1.60 and 1.84 ppm, respectively. These unusually high-field type J βCH chemical shifts are likely to arise from ring current effects. Ring current shifts for the pair of βCH resonances of Y63 and C81 are predicted from the crystal structure to be 1.32, 1.33 and 0.74, 2.33 ppm, respectively. This compares with secondary shifts of 1.32 ppm for Y63 and 1.12 ppm for C81 measured experimentally. The βCH resonances of the corresponding residues, W62 and C80, in hen lysozyme are also found to have large upfield shifts (Redfield & Dobson, 1988). Also of interest here is the fact that the spin system assigned to G48 was classified as type X in the first stage of assignment; the absence of through-bond αCH–βCH connectivities for this spin system is, however, consistent with its assignment as a glycine whose αCH resonances coincidently overlap with each other. No experimental conditions have been found that resolve the pair of resonances. G48 is the extra amino acid residue found in human lysozyme, and therefore, no comparison with hen lysozyme is possible.

(*b*) *Comparison of Hen and Human Lysozyme.* The pattern of sequential NOE effects shown in Figure 2A for human lysozyme is very similar to that found previously for hen lysozyme; for comparison, the latter is summarized in Figure 2B. Breaks in the sequential NOE pattern are found in different places for the two proteins because of differences in chemical shifts and the positions of proline residues in the two sequences. For example, the chemical shift difference of 0.23 ppm between the NH of Ala 9 (8.40 ppm) and the NH of Ala 10 (8.17 ppm) is large enough to resolve the d_{NN} connectivity in hen lysozyme. In human lysozyme, on the other hand, the chemical shift difference of 0.04 ppm between the NH of Ala 9 (8.35 ppm) and the NH of Arg 10 (8.31 ppm) is too small and the d_{NN} cross peak cannot be resolved from the diagonal, as seen in Figure 5.

Analysis of the pattern of sequential NOE effects and longer range NOE effects involving NH and αCH resonances allows a preliminary identification of secondary structure to be made (Wüthrich, 1986). The long-range NOE effects observed for human lysozyme are shown in Figure 6. Long stretches of d_{NN} connectivities are observed for residues 5–15, 26–38, and 90–102. Long-range $d_{\alpha N}(i,i+3)$ connectivities have been observed for all three segments, confirming the presence of helical secondary structure in human lysozyme as well as hen lysozyme; these are illustrated for residues 6–15 in Figure 5. Stretches of sequential $d_{\alpha N}$ connectivities are observed for residues 42–47, 50–55, and 58–61. The presence of several long-range $d_{\alpha\alpha}$, $d_{\alpha N}$, and d_{NN} connectivities between these residues, as shown in Figure 6, indicates a triple-stranded antiparallel β-sheet conformation. A second small region of antiparallel β-sheet structure is identified from long-range $d_{\alpha N}$ NOEs between residues 2 and 40 and 39 and 3, and a $d_{\alpha\alpha}$ NOE between residues 2 and 39. The long-range NOE effects

Table II: Sequence-Specific Assignments of Human Lysozyme[a]

residue	NH	αCH	βCH	γCH and others
Lys 1		3.95		
Val 2	8.84	4.85	1.98	γCH_3 1.01, 0.91
Phe 3	8.86	4.11	3.00, 2.76	δCH 7.04, εCH 7.24, ζCH 7.46
Glu 4	8.36	4.37	2.36, 2.05	
Arg 5	8.61	3.24		
Cys 6	8.91	4.74	3.19, 2.97	
Glu 7	7.87	4.13	2.62, 2.21	γCH 2.52, 2.37
Leu 8	8.47	3.66	1.58, 0.88	γCH 1.22, δCH_3 0.37, −0.26
Ala 9	8.35	4.00	1.51	
Arg 10	8.31	3.84	1.94, 1.86	
Thr 11	7.81	3.89	4.24	γCH_3 1.19
Leu 12	8.79	3.63	1.89, 0.73	γCH 1.66, δCH_3 0.61, 0.51
Lys 13	8.16	4.04	2.18, 1.92	
Arg 14	7.97	4.17	2.06	
Leu 15	7.51	4.39	1.81, 1.50	γCH 1.81, δCH_3 0.85, 0.71
Gly 16	7.55	4.08, 3.90		
Met 17	7.43	4.00	1.31	ϵCH_3 0.02
Asp 18	8.97	4.46	3.27, 2.35	
Gly 19	9.02	4.23, 3.29		
Tyr 20	7.89	4.15	3.34, 3.11	δCH 7.17, εCH 6.99
Arg 21	8.89	3.56	2.08, 1.63	γCH 2.24, 1.11, δCH 3.08, 2.96
Gly 22	7.83	4.03, 3.58		
Ile 23	7.76	3.84	2.03	γCH 1.3, γCH_3 −0.27, δCH_3 0.60
Ser 24	8.76	4.44	3.57	
Leu 25	8.83	4.24	1.97, 1.41	γCH 1.52, δCH_3 0.99, 0.97
Ala 26	8.82	3.85	1.57	
Asn 27	7.75	4.57	3.05, 2.11	
Trp 28	7.81	4.35	3.34, 3.06	N1H 9.16, C2H 6.88, C4H 6.91, C5H 6.06, C6H 6.82, C7H 7.21
Met 29	8.38	4.42	2.41, 2.28	ϵCH_3 2.09
Cys 30	8.02	2.99	3.16, 2.99	
Leu 31	8.09	3.98	2.38, 1.52	γCH 1.09, δCH_3 0.48, −0.08
Ala 32	8.38	4.07	1.40	
Lys 33	8.67	2.67	2.07, 1.47	
Trp 34	7.71	4.34	3.34, 2.80	N1H 9.72, C2H 7.78, C4H 7.72, C5H 7.17, C6H 7.26, C7H 7.58
Glu 35	8.71	4.49	2.06	
Ser 36	7.89	4.65	3.27	
Gly 37	8.12	3.75, 3.45		
Tyr 38	7.39	3.68	3.83, 3.23	δCH 6.77, εCH 6.73
Asn 39	7.13	5.50	3.49, 2.72	
Thr 40	9.18	4.04	4.46	γCH_3 1.55
Arg 41	7.65	4.49	1.68	
Ala 42	6.79	4.16	1.35	
Thr 43	8.22	5.26	3.78	γCH_3 1.12
Asn 44	8.11	5.05	2.84, 2.78	
Tyr 45	8.94	4.84	3.02, 2.81	δCH 7.16, εCH 6.59
Asn 46	8.87	4.68	2.80, 2.71	
Ala 47	8.41	3.68	1.46	
Gly 48	8.50	3.82, 3.82		
Asp 49	7.17	4.71	2.90, 2.42	
Arg 50	7.88	3.83	2.26, 2.12	
Ser 51	7.98	4.73	3.59	
Thr 52	9.03	5.03	3.84	γCH_3 0.42
Asp 53	8.87	5.25	2.68, 2.04	
Tyr 54	9.13	4.82	3.01, 2.74	δCH 7.16, εCH 6.87
Gly 55	9.07	4.53, 4.50		
Ile 56	9.21	4.11	1.23	γCH 1.21, 0.58, γCH_3 0.06, δCH_3 0.41
Phe 57	8.29	4.65		δCH 6.88, εCH 6.90, ζCH 6.65
Gln 58	7.91	3.48	2.47, 2.09	
Ile 59	7.87	4.33	1.95	γCH 1.92, 1.30, γCH_3 1.10, δCH_3 1.02
Asn 60	8.49	5.72	3.46, 3.01	
Ser 61	9.22	5.14	4.48	
Arg 62	8.75	4.18	1.77	
Tyr 63	7.31	4.34	1.62, 1.57	δCH 6.53, εCH 6.69
Trp 64	7.22	5.03	3.41, 3.34	N1H 10.27, C2H 7.68, C4H 7.62, C5H 6.72, C6H 7.22, C7H 7.30
Cys 65	7.47	5.73	2.89, 2.53	
Asn 66	8.69	5.61	2.89, 2.44	
Asp 67	10.32	4.95	3.29, 2.29	
Gly 68	8.25	4.14, 3.86		
Lys 69	8.18	4.77	1.86	
Thr 70	8.33	4.82	4.15	γCH_3 1.07
Pro 71		4.42	2.35, 1.98	δCH 4.12, 3.90
Gly 72	8.69	3.81, 3.69		
Ala 73	7.12	4.59	1.56	
Val 74	7.81	3.89	1.98	γCH_3 0.95, 0.76
Asn 75	8.71	3.80	3.12, 1.98	
Ala 76	8.36	4.04	1.48	
Cys 77	9.36	4.38	3.53, 3.47	
His 78	7.81	3.97	3.42, 3.31	δCH 7.27, εCH 8.56
Leu 79	8.70	4.72	1.66, 1.25	γCH 1.67, δCH_3 0.83, 0.80
Ser 80	8.62	5.00	3.99, 3.92	
Cys 81	8.50	3.95	1.86	
Ser 82	8.38	3.88		
Ala 83	7.81	4.34	1.67	
Leu 84	7.86	4.33	2.22	γCH 1.67, δCH_3 1.06, 0.80
Leu 85	7.17	5.61	1.78	γCH 1.72, δCH_3 1.13, 1.04
Gln 86	6.75	4.41	2.05	γCH 2.65, 2.49
Asp 87	8.69	4.22	2.64, 2.50	
Asn 88	7.39	4.90	3.02, 2.82	
Ile 89	8.27	4.60	2.13	γCH 1.31, 0.98, γCH_3 1.01, δCH_3 0.29
Ala 90	8.20	3.87	1.47	
Asp 91	9.04	4.50	2.65, 2.47	
Ala 92	7.68	3.97	1.62	
Val 93	8.62	3.26	2.18	γCH_3 0.85, 0.78
Ala 94	8.02	3.88	1.57	
Cys 95	8.29	4.94	3.36, 2.69	
Ala 96	8.82	3.77	0.87	
Lys 97	7.96	3.64		
Arg 98	7.14	4.08		
Val 99	8.29	2.46	1.88	γCH_3 −0.34, −0.58
Val 100	7.46	3.93	2.45	γCH_3 1.38, 1.11
Arg 101	7.55	4.17	2.12	
Asp 102	7.42	4.93	3.05, 2.99	
Pro 103		4.23	2.39, 1.88	δCH 3.76
Gln 104	8.45	4.11	1.95	γCH 2.34, 2.28
Gly 105	8.08	4.01, 3.90		
Ile 106	8.47	3.98	0.93	γCH 0.90, 0.21, γCH_3 −0.61, δCH_3 −0.42
Arg 107	7.31	4.10	2.21, 2.10	
Ala 108	7.24	3.84	0.91	
Trp 109	7.50	4.83	3.28, 3.22	N1H 9.90, C2H 7.35, C4H 7.84, C5H 6.61, C6H 6.86, C7H 6.99
Val 110	8.80	3.65	2.18	γCH_3 1.13, 1.04
Ala 111	8.62	4.23	1.44	
Trp 112	7.38	3.68	3.81, 3.11	N1H 9.82, C2H 6.93, C5H 6.88, C6H 7.14, C7H 7.29
Arg 113	7.75	3.76	2.23	
Asn 114	7.85	4.47	2.65, 2.61	
Arg 115	7.79	4.01	1.33	
Cys 116	7.32	4.33	2.52, 1.68	
Gln 117	6.65	3.16	1.64, 0.69	γCH 2.12
Asn 118	9.06	4.43	3.05, 2.89	
Arg 119	7.44	4.57	1.77, 1.47	1.36
Asp 120	8.43	4.73	2.90, 2.71	
Val 121	8.50	4.80	2.70	γCH_3 1.17, 0.88
Arg 122	8.27	3.96	2.03, 1.78	
Gln 123	8.67	4.06	1.90, 1.84	γCH 1.48, 1.39
Tyr 124	7.59	4.16	3.24, 2.97	δCH 7.49, εCH 6.89
Val 125	7.29	4.52	2.34	γCH_3 0.96, 0.82
Gln 126	7.38	4.20	2.10, 2.00	γCH 2.40
Gly 127	9.11	4.29, 3.86		
Cys 128	7.65	4.93	3.21, 2.71	
Gly 129	8.86	3.96, 3.89		
Leu 130	7.46	4.28	2.18	γCH_3 0.76, 0.74

[a] Chemical shifts are in ppm referenced to DSS and are accurate to ±0.02 ppm. Values are for human lysozyme at 35 °C, pH 3.8.

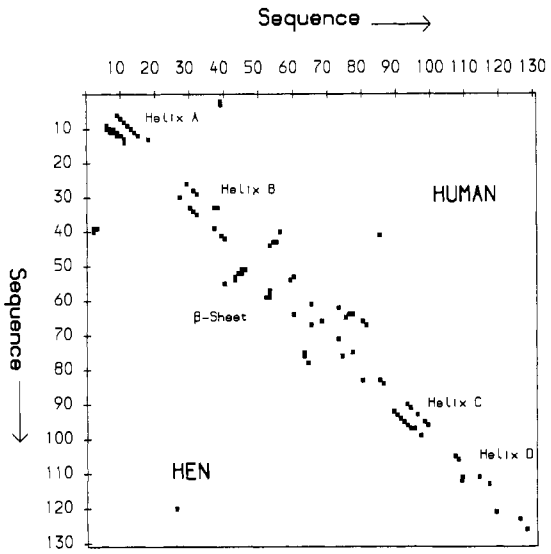

FIGURE 6: Plot showing pairs of amino acid residues for which an NOE effect involving NH or αCH protons is observed. The data for human lysozyme are displayed in the upper right side of the plot and the data for hen lysozyme in the lower left side. Regions of secondary structure are indicated.

observed between residues 62–66 and residues 73–81 are characteristic of a parallel β-sheet interaction. The long-range NOE effects identified for human lysozyme are compared in Figure 6 with those observed for hen lysozyme. The overall pattern of NOE effects observed for the two proteins is very similar, indicating that the two proteins contain the same elements of secondary structure in solution. This conclusion is fully in accord with the results of diffraction studies of the proteins in the crystalline state, which show an RMS difference of only 0.74 Å in α carbon positions (Artymiuk & Blake, 1981). There are, however, two differences in very long-range NOE effects observed for the two proteins. The $d_{\alpha N}$ connectivity observed between residues Q121 and G26 in hen lysozyme is not observed in human lysozyme; the distance between this pair of protons in the X-ray structures is 4.3 Å in hen lysozyme and 5.8 Å in human. The absence of this NOE effect in the spectrum of human lysozyme is consistent with the conformations of the two proteins in solution also differing in the region of residues 26 and 121/122. The large difference in the NH–αCH coupling constants of V120 in hen lysozyme and V121 in human, discussed in detail below, further supports the presence of a local difference in the conformations of the two proteins in solution. The $d_{\alpha\alpha}$ connectivity observed between residues R41 and L85 in human lysozyme is not observed in hen lysozyme; the distance between this pair of protons in the X-ray structures is 3.1 Å in human lysozyme and 3.3 Å in hen. This NOE effect is very weak in the spectrum of human lysozyme, and its absence in the spectrum of hen lysozyme may simply be due to the limits of the sensitivity of the experimental data. Overall, therefore, the regions of helical and β-sheet secondary structure identified for hen and human lysozymes in solution are also found in the X-ray structures of both proteins. However, an additional region of helical structure has been identified in the X-ray structures; residues 109–115 in hen and 110–116 in human form an α-helix. Sequential d_{NN} connectivities, characteristic of helical structure, have been identified for this region for both proteins in solution as shown in Figure 2. However, only a small number of long-range NOE effects, needed to confirm this type of secondary structure, have so far been identified in solution.

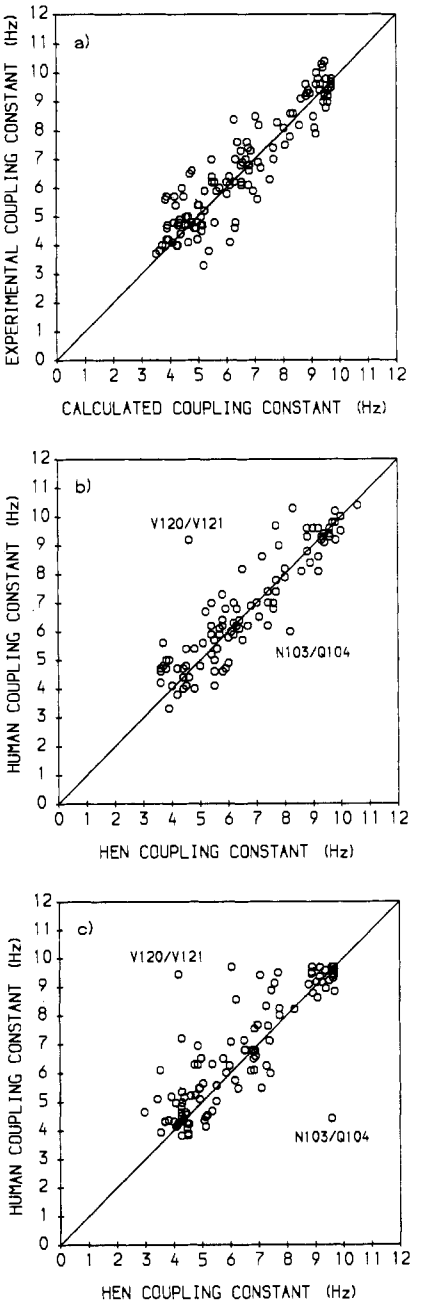

FIGURE 7: (a) Plot of the experimental NH–αCH coupling constants for human lysozyme versus the coupling constants calculated from the φ torsion angles in the X-ray structure. (b) Plot of the experimental human lysozyme coupling constants versus the experimental hen lysozyme coupling constants. (c) Plot of the human lysozyme coupling constants calculated from the φ torsion angles in the X-ray structure versus the calculated hen lysozyme coupling constants. In (b) and (c) the points corresponding to residues 120/121 and 103/104 are indicated. Stereospecific assignments for glycine αCH have not been made. The experimental glycine coupling constants are plotted against calculated coupling constants so as to give the best agreement.

A comparison of the hydrogen exchange classifications for hen and human lysozymes given in Figure 2 also shows a very similar pattern. In both proteins about 50% of the residues have amides that exchange slowly (i.e., having ≤10% exchange after 6 h at 35 °C, pH 3.8) with the solvent. These amides are located, for the most part, in the regions of helical and β-sheet secondary structure identified above. The remaining amides exchange more rapidly with solvent and are not generally located in regions of regular secondary structure. A total of 110 of the 125 residues for which amide exchange has been studied in both proteins have the same qualitative hydrogen

Table III: Coupling Constant Data for Human Lysozyme[a]

residue	J(35 °C)	J(45 °C)	J(55 °C)	J(av)	ϕ(expt) − ϕ(X-ray)	residue	J(35 °C)	J(45 °C)	J(55 °C)	J(av)	ϕ(expt) − ϕ(X-ray)
Val 2	10.3	10.0	9.9	10.0	−16	Asn 66	9.6	9.2	9.0	9.1	−6
Phe 3	7.2	7.0	7.0	7.0	−12	Asp 67	9.7		9.5	9.5	8
Glu 4	8.3	8.6	8.4	8.5	−13	Gly 68			4.1, 5.9	4.1, 5.9	
Arg 5						Lys 69	9.8	9.8	9.7	9.8	2
Cys 6	5.7	6.7	5.7	6.2	3	Thr 70	9.3	9.3	9.3	9.3	−6
Glu 7	6.0	5.0	5.8	5.4	−10	Gly 72			6.1, 6.8	6.1, 6.8	
Leu 8	≤6.6	5.8	5.6	5.7	−10	Ala 73			3.8	3.8	−2
Ala 9	5.0		4.8	4.8	−4	Val 74		8.6	8.4	8.5	7
Arg 10	4.8	4.9	5.0	5.0	1	Asn 75		6.9	7.0	7.0	11
Thr 11		5.5	5.3	5.4	−3	Ala 76			4.6	4.6	3
Leu 12	≤7.0		4.4	4.4	0	Cys 77	≤9.1	≤7.9			
Lys 13	5.1	4.7	4.7	4.7	−3	His 78	7.6	7.5	7.2	7.4	9
Arg 14	5.0	4.7	4.7	4.7	4	Leu 79	7.4	8.0	7.8	7.9	−14
Leu 15	8.1	8.4	7.8	8.1	−1	Ser 80	6.6	6.6	6.5	6.6	−14
Gly 16			6.0, 6.3	6.0, 6.3		Cys 81	5.4	4.5	4.9	4.7	3
Met 17	7.1	6.9	7.1	7.0	6	Ser 82	≤5.6	5.3	4.0	4.6	2
Asp 18	5.9			5.9	−5	Ala 83	5.0	4.9	5.6	5.2	0
Gly 19			4.8, 8.3	4.8, 8.3		Leu 84		8.4	8.7	8.6	−3
Tyr 20		5.0	5.1	5.0	−3	Leu 85	9.7	9.8	9.5	9.6	4
Arg 21	7.1	6.7	7.1	6.9	14	Ser 86	7.9	7.3		7.3	−6
Gly 22			5.8, 6.9	5.8, 6.9		Asp 87	5.2	4.7	4.6	4.6	13
Ile 23	7.7	8.1	8.1	8.1	11	Asn 88	8.5	8.3	8.4	8.4	−18
Ser 24	≤7.1	≤5.6				Ile 89		≤9.1	8.2	8.2	4
Leu 25						Ala 90	4.3		4.0	4.0	−2
Ala 26	≤6.0	5.0	3.4	4.2	6	Asp 91	3.8			3.8	13
Asn 27	7.6		7.0	7.0	−12	Ala 92	4.7	4.0	5.2	4.6	−6
Trp 28	5.3	4.9		4.9	−4	Val 93	6.0	5.5	5.3	5.4	−3
Met 29	4.7			4.7	−1	Ala 94	≤5.6		4.7	4.7	−3
Cys 30	≤6.8	4.7	5.3	5.0	−3	Cys 95	6.3	6.3	6.2	6.2	1
Leu 31		≤6.6	4.7	4.7	0	Ala 96	4.3	4.1	4.3	4.2	−3
Ala 32	≤6.4	≤6.1	4.0	4.0	2	Lys 97	4.2	≤5.4	4.4	4.4	0
Lys 33	≤6.3	≤7.3	4.2	4.2	−2	Arg 98	6.1	5.3	6.1	5.7	−12
Trp 34	6.8	6.8	6.7	6.8	0	Val 99	4.2	≤5.6	4.7	4.7	−6
Glu 35	6.4			6.4	−2	Val 100	6.6	6.7	6.7	6.7	4
Ser 36		≤11.0	10.3	10.3	13	Arg 101	7.5	7.7	7.5	7.6	−10
Gly 37			4.5, 6.6	4.5, 6.6		Asp 102	7.1	7.1	6.9	7.0	−6
Tyr 38		6.8	6.8	6.8	−1	Gln 104	5.9	5.8	6.1	6.0	−12
Asn 39	9.2	9.4	9.2	9.3	3	Gly 105			3.3, 6.1	3.3, 6.1	
Thr 40	5.2	5.8	6.0	5.9	−2	Ile 106	≤8.1	6.4	5.9	6.2	−5
Arg 41	8.6			8.6	−4	Arg 107	4.5	5.5	5.9	5.7	−15
Ala 42	≤5.9	≤5.3	4.1	4.1	0	Ala 108	3.2	4.8	4.6	4.7	−1
Thr 43	9.2	9.2	9.1	9.2	6	Trp 109	9.1	9.4	9.2	9.3	−5
Asn 44	9.4	9.4	9.3	9.4	8	Val 110			4.1	4.1	5
Tyr 45	≤9.0	7.6	8.0	7.8	4	Ala 111	3.8	≤6.2	3.7	3.7	−2
Asn 46		9.8	9.5	9.6	−9	Trp 112	≤6.7		6.5	6.5	−14
Ala 47	≤5.2	4.0	3.9	4.0	2	Arg 113	≤7.2	5.2	4.4	4.8	1
Gly 48						Asn 114	6.4			6.4	−7
Asp 49	9.7	9.8	9.6	9.7	0	Arg 115	9.0	9.5	9.4	9.4	5
Arg 50	7.4	7.4	7.2	7.3	−5	Cys 116	≤10.8	10.5	9.9	10.2	12
Ser 51	8.9	9.0	9.0	9.0	7	Gln 117	≤7.1		4.2	4.2	−3
Thr 52	9.8	9.9	9.7	9.8	9	Asn 118	7.6			7.6	11
Asp 53	9.3	9.8	9.4	9.6	−14	Arg 119	9.5		9.2	9.2	−8
Tyr 54	≤9.4	≤10.0	9.6	9.6	7	Asp 120		6.2	6.1	6.2	−2
Gly 55						Val 121	9.4	9.1	9.3	9.2	5
Ile 56	≤7.0	≤7.4	4.8	4.8	0	Arg 122	5.4	4.9	4.6	4.8	−5
Phe 57			9.8	9.8	−15	Gln 123	4.2	4.8	6.5	5.6	−14
Gln 58	≤8.7	≤7.3	6.8	6.8	0	Tyr 124	6.5	6.2	6.3	6.2	−6
Ile 59			8.2	8.2	−9	Val 125	10.8		10.4	10.4	−11
Asn 60			7.5	7.5	5	Gln 126	4.0		≤4.6	4.0	−1
Ser 61	≤6.9	≤6.5	5.6	5.6	12	Gly 127					
Arg 62	7.2	7.0	7.1	7.0	−5	Cys 128	7.3	7.5	7.4	7.4	2
Tyr 63	10.5		9.4	9.4	−2	Gly 129			4.8, 6.1	4.8, 6.1	
Trp 64	9.2	9.1	9.0	9.0	10	Val 130	9.7	9.6	9.6	9.6	−7
Cys 65	8.9	8.8	8.8	8.8	−12						

[a] Corrected coupling constants were obtained from computer fits as described under Materials and Methods; values are in hertz (Hz). The average coupling constant is the average of the 45 and 55 °C values; the 35 °C value was used if no other measurement was possible. An upper limit is given for coupling constants when poor signal-to-noise ratios prevented the use of the fitting program; these values have not been used in the analysis. Stereospecific assignments for glycine αCH have not been made. The difference in the angle ϕ is given in degrees.

exchange behavior in hen and human lysozymes. Most of the residues for which differences in hydrogen exchange classification have been observed involve a change from the intermediate category to either the slow or rapid exchange category; differences in hydrogen exchange rates are, therefore, likely to be relatively small. The factors controlling hydrogen exchange behavior are complex, and more detailed studies of the pH and temperature dependence of exchange are required before the observed differences in exchange categories can be interpreted (Pedersen et al., 1990). The similarity in hydrogen

exchange behavior, taken with the similarity of sequential and long-range NOE effects discussed above, indicates further that the two proteins have a very similar pattern of secondary structure.

Further information about the backbone conformation of the proteins in solution is provided by measurements of NH–αCH coupling constants which depend on the ϕ torsion angles (Bystrov, 1976). Coupling constants measured for human lysozyme at three temperatures, 35, 45, and 55 °C, are listed in Table III. For the majority of residues the values measured at the three temperatures agree to within 1 Hz; in cases where there are larger discrepancies almost invariably the value measured at 35 °C differs from the values at 45 and 55 °C. This arises because the line widths are greater at the lower temperature [$\Delta\nu_{1/2}$(average) is 10.4, 8.9, and 7.5 Hz at 35, 45, and 55 °C], giving rise to larger errors in the measurements particularly for small coupling constants (Neuhaus et al., 1985). In order to have as complete a set of J values as possible, the values at 45 and 55 °C were averaged and the 35 °C values were included when measurement at these higher temperatures did not prove possible. This set of coupling constants for 120 of the 130 residues of human lysozyme is also listed in Table III.

The experimental coupling constants are plotted against the coupling constants calculated by using the Karplus relationship from torsion angles defined in the X-ray structure in Figure 7a. The agreement between the two sets of data is excellent; an RMS difference of 0.79 Hz and a correlation coefficient of 0.96 are obtained. For 96 residues the agreement between the experimental and calculated coupling constants is better than 1 Hz. The residues for which worse agreement is obtained are scattered throughout the sequence. Some of the large differences, particularly for residues 101–107, correspond to residues with large temperature factors for backbone atoms in the X-ray structure; good agreement between experimental and calculated coupling constants is, however, found for some residues, for example, 72–75, where large temperature factors are also found. The observed differences cannot, therefore, simply be attributed to the effects of conformational averaging of regions of the polypeptide chain which are ill-defined in the X-ray structure. They could, however, arise from errors in the measurements of the coupling constants, from errors in the X-ray structure, or from real differences between the solution and X-ray structures. In order to explore the latter, the minimum difference in torsion angle needed to bring experimental and calculated coupling constants into exact agreement has been determined; these values are listed in Table III. A 1-Hz difference in coupling constant corresponds to a difference of 22° in torsion angle for ϕ in the region of −120°, characteristic of extended structure, and to a difference of 8° in torsion angle for ϕ in the region of −60°, characteristic of helical structure. For 82 residues the required difference in torsion angle is less than 10°, and for only 2 residues is the difference more than 15°. Thus even without consideration of experimental error only very small differences need to exist between the average structures of human lysozyme in the crystalline and solution states to explain the deviations from a perfect correlation in Figure 7a.

Similar coupling constant measurements have been made for hen lysozyme (Smith, Sutcliffe, Redfield, and Dobson, unpublished data). There are 97 residues for which measurements have been made in both proteins, and the measured coupling constants for the two proteins are compared in Figure 7b. An RMS difference of 0.90 Hz and a correlation coefficient of 0.90 are obtained from the experimental data; these values are essentially identical (RMS 0.91 Hz, correlation coefficient 0.90) if comparison only of the conserved residues is made. The coupling constants calculated from the X-ray structures for the same 97 residues are compared in Figure 7c; in this case an RMS difference of 1.20 Hz and a correlation coefficient of 0.82 are obtained. It is clear from a comparison of panels b and c of Figure 7 that the ϕ angles for hen and human lysozymes in solution are even more similar than would be expected from a comparison of the X-ray structures of the two proteins. There is one residue, V120/V121, for which the experimental coupling constant differs significantly between the two proteins in solution; the observed difference in coupling constant of 4.6 Hz corresponds to a difference in ϕ of at least 41°. The ϕ torsion angle of this residue in the two crystal structures differs by 49°. Thus, this particular feature appears to be common to the two states. Other large differences predicted in the X-ray structures are not, however, observed in solution. The coupling constants of residue N103 in hen and Q104 in human are predicted on the basis of the X-ray structures to differ by 5.2 Hz; the observed difference in coupling constant is only 2.2 Hz.

If the coupling constant of V121 is ignored, then an RMS difference of 0.77 Hz between hen and human lysozyme experimental coupling constants is obtained. This value is similar to the value obtained above for the comparison of the experimental and X-ray data for human lysozyme and indicates that with the exception of V121 the backbone structures of hen and human lysozymes in solution are as similar to each other as are the structures of human lysozyme in the solution and solid states. The RMS difference of 0.77 Hz may well represent the limit that can be obtained given the errors in experimental measurements of coupling constants and the limits of X-ray data at 1.5-Å resolution.

NH and αCH chemical shift values are obtained directly from 2-D NMR spectra; they are, therefore, the easiest parameter to measure quantitatively. Inspection of the fingerprint region of the COSY spectrum of human lysozyme in Figure 1 shows the large range of chemical shifts observed for the NH and αCH resonances of human lysozyme; the NH resonances fall over a range of 3.7 ppm and the αCH resonances over a range of 3.3 ppm. This is in contrast to smaller chemical shift ranges of 0.7 and 0.8 ppm found for the NH and αCH resonances of the amino acids in random coil tetrapeptides (Bundi & Wüthrich, 1979). The large range of chemical shifts found for human lysozyme is the result of a variety of interactions which are present in the 3-D structure of the protein. It is not yet possible to rationalize fully observed chemical shift values in terms of features of protein structures; unlike the NOE effects and coupling constants, chemical shift values do not depend on well-defined pairwise interactions but involve summations of contributions from a variety of sources. The availability of values for hen and human lysozymes, however, enables an attempt to be made here to correlate the observed chemical shift differences with structural features of the two proteins.

The secondary, or conformational dependent, shifts are determined by subtracting random coil values from the experimental shifts; a positive secondary shift indicates a downfield shift and a negative value an upfield shift. Secondary shifts for NH and αCH resonances of human lysozyme are plotted as a function of sequence in Figure 8a; large shifts are found for residues throughout the human lysozyme sequence. There are 20 NH protons and 7 αCH protons with shifts of greater than 1 ppm and 42 NH protons and 32 αCH protons with shifts of between 0.5 and 1.0 ppm. The average magnitude of secondary shifts is 0.56 ppm for NH resonances and 0.40 ppm for αCH resonances. These large secondary

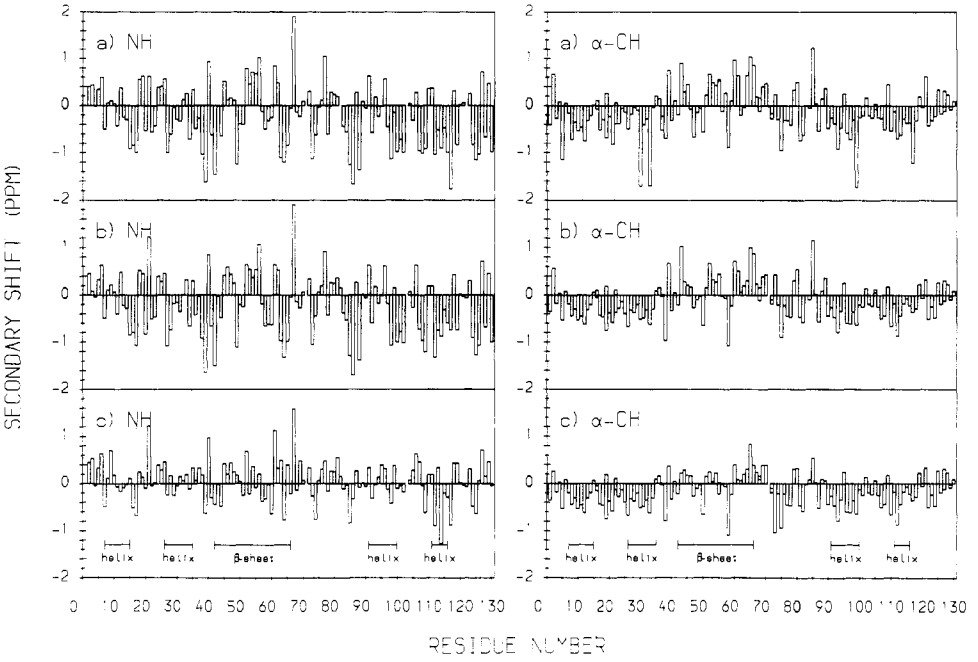

FIGURE 8: Plot of experimental secondary shift versus amino acid residue number for the NH and αCH protons of human lysozyme. (a) The random coil shifts have been subtracted from the experimental chemical shifts. (b) The random coil shifts and ring current shifts have been subtracted from the experimental chemical shifts. (c) The random coil shifts, ring current shifts, and contributions from nearby oxygen atoms have been subtracted from the experimental chemical shifts. Regions of secondary structure are indicated.

shifts are likely to arise from specific interactions in the protein resulting from the close proximity in the globular structure of side-chain or other main-chain atoms to the NH and αCH protons. The analysis of NOE effects, hydrogen-bonding patterns, and spin–spin coupling constants detailed above has shown that the structure of human lysozyme in solution is very similar to the structure in the crystalline state. If the X-ray coordinates of human lysozyme are assumed to give a good description of the structure in solution, then it is possible to use these coordinates to calculate some of the contributions to chemical shifts arising from aromatic rings and oxygen atoms in the protein.

Human lysozyme contains 14 aromatic amino acid residues, and large shifts resulting from the presence of the aromatic rings are calculated to affect many residues. These have been subtracted from the secondary shifts shown in Figure 8a to give a new set of secondary shifts which are plotted as a function of sequence in Figure 8b. It is clear from a comparison of panels a and b of Figure 8 that ring current shifts are predicted to make a significant contribution to the chemical shifts of several αCH protons; the secondary shifts of the αCH protons of R5, C30, K33, V99, and Q117 are reduced by as much as 1 ppm when the ring current effects are considered. The effect on the secondary shifts of NH protons is less pronounced; only 1 of the 20 secondary shifts of greather than 1 ppm results from ring current shifts. Thus, ring current shifts do not by themselves explain the large range of secondary shifts observed in the spectrum of human lysozyme.

Pardi, Wagner, and Wüthrich (Pardi et al., 1983) have found a correlation between the NH and αCH chemical shifts of BPTI and the distance to nearby oxygen atoms in the X-ray structure (excluding oxygen atoms of residues i or $i + 1$); downfield shifts correspond to short H–O distances while upfield shifts correspond to longer H–O distances. Human lysozyme has 91 NH protons that are located within 3.0 Å of an oxygen atom in the X-ray structure; 77 of these oxygens belong to a backbone carbonyl group, 6 belong to internal side-chain oxygens, and the remaining 8 are from water molecules; oxygen atoms on exposed side chains have not been included in the calculation. A correlation coefficient of 0.76 is found between the secondary shifts of the 91 NH resonances and the inverse cube of the distance to the oxygen atom. This correlation coefficient is closely similar to the value of 0.75 obtained from the analysis of the BPTI data (Pardi et al., 1983; Wagner et al., 1983). The best fit line has a slope of 15.5 and an intercept of −2.15 for the lysozyme data compared to values of 19.2 and −2.3 for BPTI; the relatively small difference in the slope could result simply from a difference in the method of generating hydrogen atom positions from the heavy atom positions in the X-ray structure. Human lysozyme has 24 αCH protons that are located within 3.5 Å of an oxygen atom in the X-ray structure; a correlation coefficient of 0.57 is found between the secondary shifts of the corresponding resonances and the inverse cube of the distance to the oxygen atom. This correlation coefficient is substantially worse than the value of 0.76 obtained from the BPTI data. The best fit line has a slope of 14.7 and an intercept of −0.6 for the lysozyme data compared to values of 19.6 and −0.7 for BPTI. The poorer fit for lysozyme could arise because many of the αCH protons close to oxygen atoms are not found in regular β-sheet structure in contrast to the situation in BPTI. The overall result of the present analysis, however, supports the idea, first suggested for BPTI (Pardi et al., 1983), that a relatively simple expression can go some way to rationalizing the observed main-chain shifts.

The parameters obtained from the human lysozyme fits have been used to calculate the contributions from nearby oxygen atoms to individual NH and αCH chemical shifts. The secondary shifts corrected for these contributions are plotted as a function of sequence in Figure 8c. The effect of making these corrections to the secondary shift of the NH resonances is fairly dramatic; the average NH secondary shift decreases from 0.56 to 0.33 ppm. The number of NH resonances with secondary shifts greater than 1 ppm decreases from 20 to 4, and the number with shifts between 0.5 and 1.0 ppm decreases from 40 to 19. Of the 87 NH secondary shifts greater than 0.3 ppm, 16 protons have no oxygen atom within 3.0 Å; their secondary shifts cannot be explained by this mechanism. For the re-

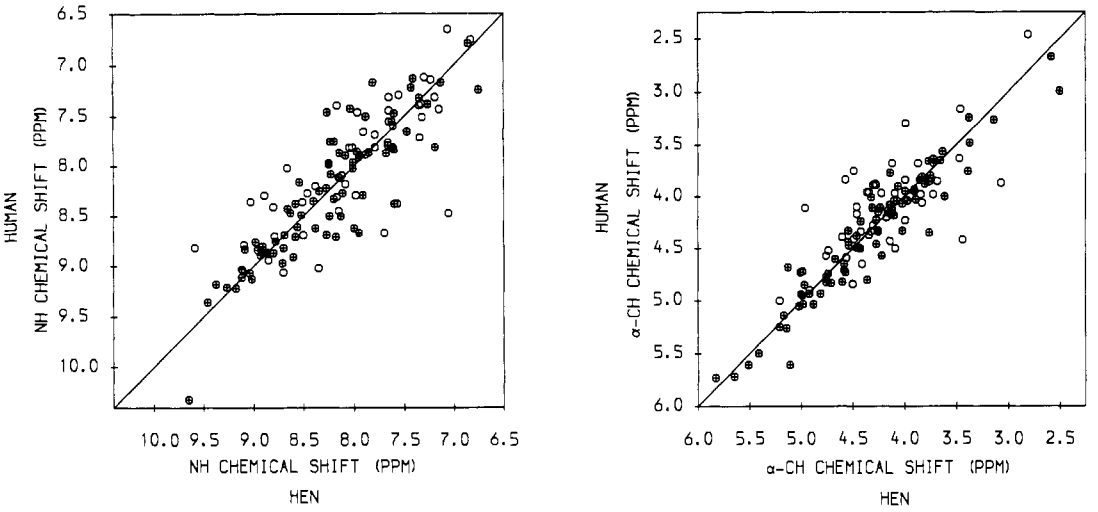

FIGURE 9: Comparison of NH and αCH chemical shift values for hen and human lysozymes. Conserved residues are indicated by the crossed circles; substituted residues, by the open circles.

mainder, however, the residual secondary shifts of 60 resonances are decreased by at least 0.1 ppm when the contribution from oxygen atoms is considered; the secondary shifts of only 8 of the 87 NH resonances are made worse by considering this contribution, and in no case is this effect substantial. The effect on the αCH chemical shifts is predictably less dramatic; the average secondary shift decreases from 0.34 to 0.30 ppm. Of the 67 αCH secondary shifts greater than 0.3 ppm only 13 are decreased by at least 0.1 ppm when the contribution from oxygen atoms is considered; 49 of the residues have no oxygen atom within 3.5 Å. The shift contributions from oxygen, however, account to a large extent for the secondary shifts of several of the downfield-shifted αCH resonances, including those of T43, S61, and L85. By contrast, they have very little effect on the secondary shifts of upfield-shifted resonances, many of which correspond to residues in helical regions of secondary structure as shown in Figure 8c. Dalgarno et al. (1983) have proposed a correlation between the αCH secondary shift and the torsion angle ψ; residues in helical regions of secondary structure ($\psi = -60°$) have upfield-shifted αCH resonances, and residues in β-sheet regions ($\psi = +120°$) have downfield-shifted resonances. C95 is the only residue located in helical secondary structure in human lysozyme which does not have an upfield-shifted αCH resonance. Although there appears to be a correlation between upfield-shifted αCH resonances and helical secondary structure, we have not been able to find a specific correlation between the ψ torsion angle and the magnitudes of the upfield shifts observed for human lysozyme. In addition, there are several upfield-shifted resonances, Q58, for example, which have ψ values that are much larger than −60°.

Like the NH and αCH secondary shifts of human lysozyme, those of hen lysozyme also show a correlation with the inverse cube of the distance to nearby oxygen atoms; the correlation coefficients obtained for the NH and αCH shifts are 0.54 and 0.57, respectively. The poorer correlation obtained for the NH shifts compared to that obtained for human lysozyme or BPTI could be the result of a poorer resolution X-ray structure; the hen lysozyme X-ray structure was obtained at 2.0-Å resolution whereas those of human lysozyme and BPTI were obtained at 1.5- and 1.4-Å resolution, respectively. Nevertheless, if the parameters obtained from the human lysozyme fit are used to calculate the contribution from nearby oxygen atoms to the hen lysozyme secondary shifts, then the number of secondary shifts greater than 0.5 ppm is decreased from 70 to 39 and from 42 to 28 for the NH and αCH resonances, respectively.

The secondary shifts observed for the NH and αCH resonances of human and hen lysozymes can therefore be rationalized, in part, by considering features of the protein structure including the position of aromatic rings and the proximity of oxygen atoms to the NH and αCH protons. It is of interest to see whether *differences* between the chemical shifts of the two proteins can be explained in terms of *differences* between the structures of the two proteins. The NH and αCH chemical shift values of hen and human lysozymes are compared in Figure 9; this reveals that the correlation between them is good over the entire chemical shift range. An RMS difference of 0.35 ppm and a correlation coefficient of 0.86 are obtained for the amide shifts and an RMS difference of 0.27 ppm and a correlation coefficient of 0.89 for the αCH resonances. This confirms the significance of the main-chain structure in determining the shift values. The plot of chemical shift differences as a function of residue number (Figure 10a) indicates that there are, however, large differences between the shifts in the two proteins and that these are found both in regions of regular secondary structure and in regions of less well-defined secondary structure. Figures 9 and 10a show that the largest differences in chemical shift are found for substituted as compared to conserved residues. Comparison of the chemical shift values indicates RMS differences of 0.30 and 0.19 ppm, respectively, for the NH and αCH resonances of conserved residues and values of 0.41 and 0.36 ppm for those resonances of substituted residues. The larger RMS difference for substituted residues could be due to differences in the random coil NH and αCH chemical shift values for different amino acid residues (Bundi & Wüthrich, 1979). Correction for the random coil shifts lead to a significant improvement in the correlation for αCH resonances but in fact to a worsening in the agreement for the NH resonances (RMS differences of 0.45 and 0.28 ppm are obtained for NH and αCH resonances of substituted residues, respectively). The sequences of hen and human lysozymes differ at several aromatic amino acid positions; substitutions at positions 15, 23, 45, and 57 involve the removal or introduction of an aromatic residue whereas substitutions at positions 34, 38, 63, and 124 involve the change of one aromatic residue to another. Differences of up to ±0.5 ppm are found in the predicted ring current shifts for resonances of hen and human lysozymes; these can be attributed to amino acid substitutions involving aromatic residues along with small structural rearrangements. Correction for these predicted differences in ring current shifts leads to an improvement in the chemical shift correlation for

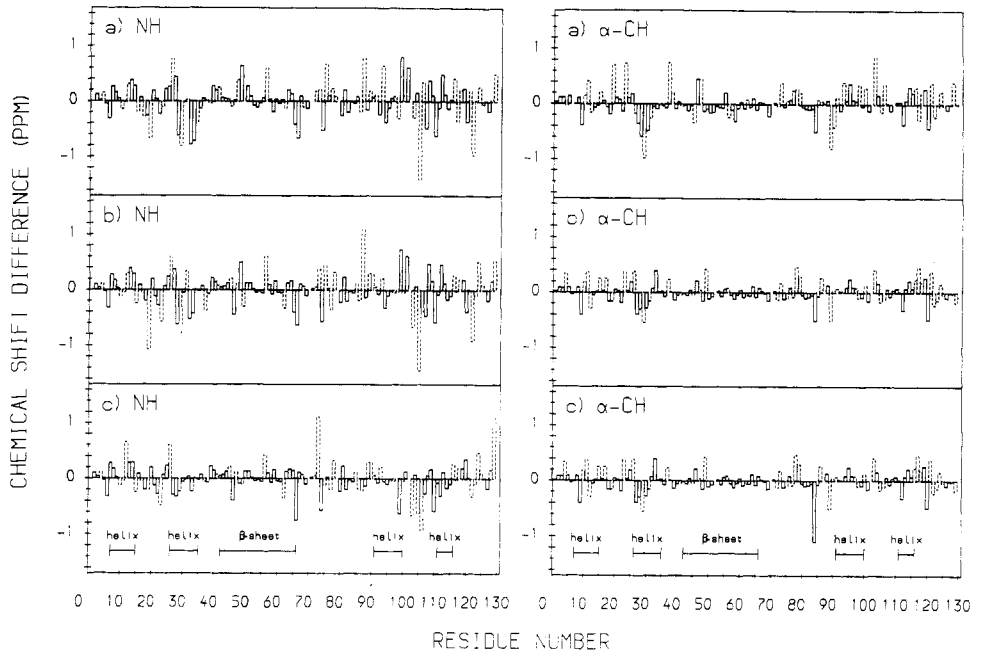

FIGURE 10: Plot of chemical shift differences (hen − human) versus amino acid residue number for the NH and αCH resonances. Conserved residues are indicated by solid lines and substituted residues by broken lines. (a) Comparison of uncorrected experimental chemical shifts. (b) Comparison of experimental chemical shifts corrected for random coil shifts and ring current shifts. (c) Comparison of experimental chemical shifts corrected for random coil shifts, ring current shifts, and contributions from nearby oxygen atoms. Only those chemical shifts that differ in the two proteins by more than 0.3 ppm have been corrected for the contribution from oxygen. A correlation coefficient of 0.70 is found between the NH chemical shift differences of greater than 0.3 ppm and the difference in the inverse cubes of the distances to oxygen atoms in the two structures. Regions of secondary structure identified by NMR are indicated.

many residues in the region of the aromatic substitutions, as shown in Figure 10b. For example, the chemical shift difference for the NH of K33 decreases from −0.72 ppm to −0.45 ppm when the change in ring current shift contribution resulting from the replacement of F34 in hen lysozyme by W34 in human lysozyme is taken into account. The chemical shift difference for the αCH of T47 decreases from 0.44 to 0.04 ppm when the additional ring current shift contribution resulting from the substitution of tyrosine in human lysozyme for arginine at position 45 in hen lysozyme is taken into account. However, only a small improvement is found for the overall correlation of hen and human lysozyme chemical shifts; an RMS difference of 0.35 ppm is found for the NH resonances and of 0.19 ppm for the αCH resonances. Thus, differences in ring current shifts do not appear to be make a significant contribution to the overall difference in chemical shifts between the two proteins. Indeed, after differences in random coil and ring current shifts have been taken into account, there are still 41 NH chemical shifts and 18 αCH chemical shifts for which differences of greater than 0.3 ppm are found between the two proteins.

Comparison of NH–O and αCH–O distances for the hen and human lysozyme X-ray structures shows that many of these distances differ by more than 0.1 Å. An increase in an NH–O distance from 1.8 to 1.9 Å would be expected to lead to a 0.4 ppm upfield shift of the NH resonance. There are 84 NH resonances and 111 αCH resonances for which the chemical shift values in the two proteins differ by less than 0.3 ppm after correction for random coil and ring current shift differences have been made. For many of these NH and αCH protons the distance to the closest oxygen atom in the two X-ray structures differs by 0.1 Å or more. The very small differences in chemical shifts for so many residues of hen and human lysozyme indicate that the structures in solution may be even more similar than would be predicted from a comparison of their X-ray structures; this is in agreement with the results of the coupling constant analysis presented above. There are, however, 18 αCH resonances and 41 NH resonances for which the chemical shift values in the two proteins differ by more than 0.3 ppm. The observed chemical shift differences for these resonances could be the result of significant differences in the distance to oxygen atoms in the two protein structures. The difference in distances between αCH protons and oxygen atoms in the two structures does not explain differences in the experimental αCH chemical shifts. Only one of the 18 αCH resonances with shift differences greater than 0.3 ppm is within 3.5 Å of an oxygen atom in either structure. By contrast, the chemical shift differences of 28 of these 41 NH resonances are decreased when differences in the distances to oxygen atoms are considered; the shift difference is increased for only 6 of the 41 residues. Seven of the 41 residues to not have an oxygen atom within 3.0 Å in either X-ray structure. When the differences in distances to oxygen are taken into account for these 41 NH resonances, the overall RMS difference between hen and human NH chemical shifts decreases from 0.35 to 0.29 ppm. The corrected shift difference for both the NH and αCH resonances is plotted as a function of sequence in Figure 10c. Thus, many of the large NH shift differences between hen and human lysozyme seem to be the result of differences in the distances to oxygen atoms in the two structures. For example, the −1.07 ppm shift difference between the NH resonance of G19 in human lysozyme and N19 in hen lysozyme decreases to −0.20 when the −0.29-Å difference in the distance to the backbone oxygen of residue 23 is taken into account. The −1.45 ppm shift difference between the NH of I106 in human and the NH of M105 in hen decreases to −0.63 ppm when the hydrogen-bonding pattern is considered. The NH of M105 in hen lysozyme is hydrogen bonded to the side-chain OH group of Y23 (d_{NH-O} = 2.27 Å). In human lysozyme this tyrosine is replaced by an isoleucine and the hydrogen bond is no longer possible. However, the chemical shift difference of three resonances, R73/V74 NH, L84/L85 αCH, and L129/V130 NH, is increased significantly when the differences in the

distance to oxygen atoms are considered. The chemical shifts of R73 NH, L84 αCH, and L129 NH in hen lysozyme and V74 NH in human lysozyme are not explained by taking the distance to the nearby oxygen atoms into account; in fact, the secondary shifts of these resonances are increased rather than decreased by the oxygen contribution. Thus, it is not surprising that differences in the chemical shifts of these resonances cannot be explained by differences in these contributions. For these residues other factors, which are not as yet fully understood, must contribute to the observed chemical shifts.

Conclusion

Using 2-D NMR techniques, it has been possible to assign all the backbone resonances in the spectrum of human lysozyme. Comparison of the NOE, hydrogen exchange, and main-chain coupling constant data for hen and human lysozymes shows that these are closely similar for the two proteins. This confirms for the solution state the crystallographic result that the two proteins have very similar backbone conformations despite sequences that differ by 40%. The chemical shift values for the resonances of main-chain atoms also show a high degree of correlation, even for nonconserved residues, and indicate the dominance of the main-chain conformation in determining the shift values. Large chemical shift differences (up to 1 ppm) between hen and human lysozymes, however, occur even for main-chain resonances of conserved residues; in many cases these appear to reflect conformational differences that are very small and are at the limit of the resolution of a crystallographic structure at a resolution of 2.0 Å. Indeed, attempts to interpret in more detail the chemical shift differences between the two proteins by examination of their crystal structures have had only limited success. Such an analysis is, however, restricted by our present understanding of the origin of chemical shift effects in proteins. Nevertheless, the results indicate that considerable caution must be exercised in interpreting large chemical shift changes as evidence for significant structural differences associated with amino acid substitutions in proteins. Despite the limitations of the interpretation of the chemical shift data, the empirical correlations observed in the present work are such as to suggest that combining shift data with NH exchange, coupling constants, and NOE effects might be of considerable value in strategies to assign the spectra of proteins on the basis of existing assignments for homologous proteins.

Acknowledgments

We thank N. Soffe and J. Boyd for their assistance. We acknowledge J. Blazer for her preliminary work on the human lysozyme coupling constants. C.R. acknowledges Lady Margaret Hall, University of Oxford, for an E.P.A. Cephalosporin Junior Research Fellowship. This work is a contribution from the Oxford Centre for Molecular Sciences.

Supplementary Material Available

A table listing secondary shifts, calculated ring current shifts, and calculated shift contributions from nearby oxygen atoms for the NH and αCH resonances of human lysozyme (8 pages). Ordering information is given on any current masthead page.

Registry No. Lysozyme, 9001-63-2.

References

Anil Kumar, Ernst, R. R., & Wüthrich, K. (1980) *Biochem. Biophys. Res. Commun. 95*, 1–6.

Archer, D. B., Jeenes, D. J., MacKenzie, D. A., Brightwell, G., Lambert, N., Lowe, G., Radford, S. E., & Dobson, C. M. (1990) *Biotechnology* (in press).

Artymiuk, P. J., & Blake, C. C. F. (1981) *J. Mol. Biol. 152*, 737–762.

Aue, W. P., Bartholdi, E., & Ernst, R. R. (1976) *J. Chem. Phys. 64*, 2229–2246.

Bax, A., & Freeman, R. (1981) *J. Magn. Reson. 44*, 542–561.

Bax, A., & Davies, D. G. (1985) *J. Magn. Reson. 65*, 355.

Bax, A., & Drobny, G. P. (1985) *J. Magn. Reson. 61*, 306–320.

Blake, C. C. F., Mair, G. A., North, A. C. T., Phillips, D. C., & Sarma, V. R. (1967) *Proc. R. Soc. London, B 167*, 365–377.

Boyd, J., Dobson, C. M., & Redfield, C. (1985) *Eur. J. Biochem. 153*, 383–396.

Bundi, A., & Wüthrich, K. (1979) *Biopolymers 18*, 285–297.

Bystrov, V. F. (1976) *Prog. NMR Spectrosc. 10*, 41–81.

Chazin, W. J., & Wright, P. E. (1988) *J. Mol. Biol. 202*, 623–636.

Dalgarno, D. C., Levine, B. A., & Williams, R. J. P. (1983) *Biosci. Rep. 3*, 443–452.

Driscoll, P. C.; Hill, H. A. O., & Redfield, C. (1987) *Eur. J. Biochem. 170*, 279–292.

Eich, G., Bodenhausen, G., & Ernst, R. R. (1982) *J. Am. Chem. Soc. 104*, 3731–3732.

Gao, Y., Lee, D. J., Williams, R. J. P., & Williams, G. (1989) *Eur. J. Biochem.* (in press).

Giessner-Prettre, C., & Pullman, B. (1969) *C. R. Seances Acad. Sci., Ser. D 268*, 1115–1117.

Griesenger, C., Sorensen, O. W., & Ernst, R. R. (1987) *J. Magn. Reson. 75*, 474–492.

Handoll, H. (1985) D. Phil. Thesis, University of Oxford.

Hoch, J. C. (1983) Ph.D. Thesis, Harvard University.

Hoch, J. C., Dobson, C. M., & Karplus, M. (1982) *Biochemistry 21*, 1118–1125.

Imoto, T., Johnson, L. N., North, A. C. T.; Phillips, D. C., & Rupley, J. A. (1972) in *The Enzymes* (Boyer, P. D., Ed.) 3rd ed., Vol. 7, pp 665–868, Academic, New York.

Jeener, J., Meier, B. H., Bachmann, P., & Ernst, R. R. (1979) *J. Chem. Phys. 71*, 4546–4553.

Johnson, C. E., & Bovey, F. A. (1958) *J. Chem. Phys. 29*, 1012–1014.

Karplus, M. (1959) *J. Phys. Chem. 30*, 11–15.

Kikuchi, M., Yamamoto, Y., Taniyama, Y., Ishimaru, K., Yoshikawa, W., Kaisho, Y., & Ikehara, M. (1988) *Proc. Natl. Acad. Sci. U.S.A. 85*, 9411–9415.

Macura, S., Huang, Y., Suter, D., & Ernst, R. R. (1981) *J. Magn. Reson. 43*, 259–281.

Marion, D., & Wüthrich, K. (1983) *Biochem. Biophys. Res. Commun. 113*, 967–974.

Muraki, M., Morikawa, M., Jigami, Y., & Tanaka, H. (1987) *Biochim. Biophys. Acta 916*, 66–75.

Muraki, M., Morikawa, M., Jigami, Y., & Tanaka, H. (1989) *Eur. J. Biochem. 179*, 573–579.

Neuhaus, D., Wagner, G., Vasak, M., Kagi, J. H. R., & Wüthrich, K. (1985) *Eur. J. Biochem. 151*, 257–273.

Otting, G., & Wüthrich, K. (1987) *J. Magn. Reson. 75*, 546–549.

Pardi, A., Wagner, G., & Wüthrich, K. (1983) *Eur. J. Biochem. 137*, 445–454.

Pardi, A., Billeter, M., & Wüthrich, K. (1984) *J. Mol. Biol. 180*, 741–751.

Pedersen, T. G., Sigurskjold, B. W., Andersen, K. V., Kjaer, M., Poulsen, F. M., Dobson, C. M., & Redfield, C. (1989)

Biochemistry (submitted for publication).
Press, W. H., Flannery, B. P., Teukolsky, S. A., & Vetterling, W. T. (1986) *Numerical Recipes*, pp 289–293, Cambridge University Press, Cambridge.
Redfield, C., & Dobson, C. M. (1988) *Biochemistry 27*, 122–136.
States, D. J., Haberkorn, R. A., & Ruben, D. J. (1982) *J. Magn. Reson. 48*, 286–292.
Torchia, D. A., Sparks, S. W., & Bax, A. (1989) *Biochemistry 28*, 5509–5524.
Wagner, G., Pardi, A., & Wüthrich, K. (1983) *J. Am. Chem. Soc. 105*, 5948–5949.
Wand, A. J., DiStefano, D. L., Feng, Y., Roder, H., & Englander, S. W. (1989) *Biochemistry 28*, 186–194.
Wüthrich, K. (1986) *NMR of Proteins and Nucleic Acids*, Wiley, New York.

Determination of the Conformation of d(GGAAATTTCC)$_2$ in Solution by Use of ^{1}H NMR and Restrained Molecular Dynamics†

Masato Katahira,‡ Hiromu Sugeta, and Yoshimasa Kyogoku*
Institute for Protein Research, Osaka University, Suita, Osaka 565, Japan
Satoshi Fujii
Faculty of Pharmaceutical Sciences, Osaka University, Suita, Osaka 565, Japan
Received January 4, 1990; Revised Manuscript Received April 18, 1990

ABSTRACT: The conformation of the putative bent DNA d(GGAAATTTCC)$_2$ in solution was studied by use of ^{1}H NMR and restrained molecular dynamics. Most of the resonances were assigned sequentially. A total of 182 interproton distance restraints were determined from two-dimensional nuclear Overhauser effect spectra with short mixing times. Torsion angle restraints for each sugar moiety were determined by qualitative analysis of a two-dimensional correlated spectrum. Restrained molecular dynamics was carried out with the interproton distances and torsion angles incorporated into the total energy function of the system in the form of effective potential terms. As initial conformations for restrained molecular dynamics, classical A-DNA and B-DNA were adopted. The root mean square deviation (rmsd) beteween these two conformations is 5.5 Å. The conformations obtained by use of restrained molecular dynamics are very similar to each other, the rmsd being 0.8 Å. On the other hand, the conformations obtained by use of molecular dynamics without experimental restraints or restrained energy minimization depended heavily on the initial conformations, and convergence to a similar conformation was not attained. The conformation obtained by use of restrained molecular dynamics exhibits a few remarkable features. The second G residue takes on the BII conformation [Fratini, A. V., Kopka, M. L., Drew, H. R., & Dickerson, R. E. (1982) *J. Biol. Chem. 257*, 14686–14707] rather than the standard BI conformation. There is discontinuity of the sugar puckering between the eighth T and ninth C. The minor groove of the oligo(dA) tract is rather compressed. As a result, d(GGAAATTTCC)$_2$ is bent.

It has been demonstrated that DNAs which contain an oligo(dA) tract are bent, by means of electrophoresis (Wu & Crothers, 1984; Hagerman, 1985, 1986; Koo et al., 1986; Haran & Crothers, 1989) and electron microscopy (Griffith et al., 1986). Several models for DNA bending have been proposed (Koo et al., 1986; Ulanovsky & Trifonov, 1987; Burkhoff & Tullius, 1987; Koo & Crothers, 1988; Calladine et al., 1988), but they are contradictory. Crystallographic studies (Nelson et al., 1987; Coll et al., 1987; DiGabriele et al., 1989) and spectroscopic studies (Roy et al., 1987; Kintanar et al., 1987; Katahira et al., 1988; Sarma et al., 1988; Patapoff et al., 1988; Leroy et al., 1988; Nadeau & Crothers, 1989; Celda et al., 1989) on DNAs containing the oligo(dA) tract were performed, but the correlation between the oligo(dA) tract and DNA bending remained unclear, although conformational deviations were reported in some of the papers.

To clarify the correlation, we have performed an NMR[1] study on the conformation of d(GGAAATTTCC)$_2$. When it was repeated in a synthetic polymer, macroscopic bending of the molecule was observed in an electrophoretic study (Hagerman, 1985). Thus, remarkable conformational features related to macroscopic bending are expected to be found in it with NMR spectroscopy. The conformation of d(GAAAATTTTC)$_2$, whose sequence is very similar to our molecule, has been already studied, and a conformational junction at the central AT sequence was suggested (Sarma et al., 1988). Our molecule has two base pairs at both ends, before and after the oligo(dA) tract. Therefore, it is expected

† This work was supported by a grant from the Ministry of Education, Science and Culture of Japan. M.K. was partly supported by grants from the Japan Society for the Promotion of Science for Japanese Junior Scientists and the CIBA-GEIGY Foundation for the Promotion of Science, Takarazuka, Japan.
‡ Present address: Department of Chemistry, University of Utrecht, Paduallaan 8, 3584 CH Utrecht, The Netherlands.

[1] Abbreviations: NMR, nuclear magnetic resonance; NOE, nuclear Overhauser effect; NOESY, two-dimensional NOE spectroscopy; DQF-COSY, two-dimensional double quantum filtered correlated spectroscopy; rmsd, root mean square deviation.

0006-2960/90/0429-7214$02.50/0